Thermal Performance of Eccentric High-Temperature Latent Heat Storage System: Passive Heat Transfer Enhancement Strategy

Alok K. Ray[1], Dibakar Rakshit[2*], K. Ravi Kumar[2], Hal Gurgenci[3]

1- University of Queensland and IIT Delhi Academy of Research,Indian Institute of Technology, Delhi (India)

2-Department of Energy Science and Engineering, Indian Institute of Technology, Delhi (India)

3-School of Mechanical and Mining Engineering,University of Queensland (Australia)

Abstract

The present study demonstrates the combined influence of orientation of latent heat storage (LHS) domain and radial eccentricity of the heat transfer fluid (HTF) tube on the charging characteristics of high-temperature LHS system with help of a comprehensive numerical investigation. Charging duration of concentric horizontal configuration (e_x= e_y= 0, θ = 0°) is found to be 19.94 % lower than the vertical domain (e_x= e_y = 0, θ = 90°). Thereafter, three vertical radial eccentricity of HTF tube is considered for the domain θ = 0°. The spatio-temporal distribution of melting fraction and temperature during phase change are observed for both concentric and eccentric LHS domain. Degree of eccentricity in horizontal direction (e_x = 5 mm and 10 mm) does not produce significant variation as compared to concentric (e_x = e_y = 0) configuration. However, charging duration for the LHS domain having vertical eccentricity (e_y = -5 mm, θ = 0°) is observed to be 11.7 % lower than concentric domain.Furthermore, the charging duration for e_y = -10 mm is 17.64 % and 33.33% lower than θ = 0° and θ = 90° respectively.

Keywords: High-temperature, PCM, LHS, HTF, Eccentricity, Orientation

1. Introduction

Solar energy is one of the most abundant sustainable energy resources available to be harnessed. Solar thermal and Solar photovoltaic are the two technologies to convert solar energy to electrical energy. However, the spatial and temporal variability is a major bottleneck against wide-scale utilization of solar technology. Efficient storage solutions are paramount to address the intermittency problem and can result in higher dispatchability of solar power (Zablocki,2019). LHS technology involves three distinct stages as presented in Figure *1*. Utilizing high-temperature PCMs for LHS systems can provide numerous benefits such as high thermal stability, high storage density, and high exergetic efficiency (Robinson,2017). Hence, high-temperature LHS coupled to a high-temperature heat engine can be considered as a potential alternative for storing solar energy during the daylight hours and releasing the accumulated energy during periods without sunlight (Ray, 2021).

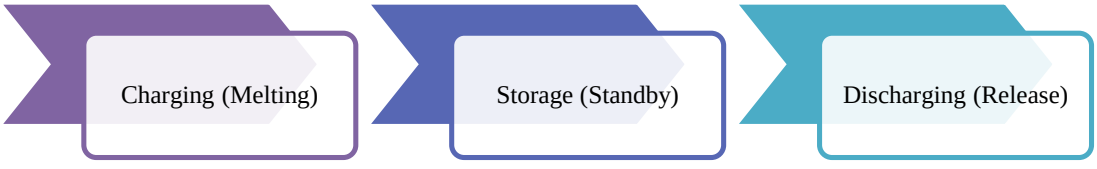

Figure 1:Three different stages of latent heat storage system

The major challenge for latent heat storage systems is that low thermal conductivity of the PCMs results in a low energy accumulation/release rate (Nazir, 2019). There are different heat transfer enhancement strategies to address this challenge (Jegadheeswaran, 2009). Active strategy involves use of metal based matrix and foams, nanoparticles, fins, cascaded arrangement, and encapsulation. However, adding fins, metal matrix and foams reduces the volume of PCM results loss in storage/release capacity (Al-Maghalseh, 2018). Passive enhancement includes change in place of HTF tube and variation in the orientation of the LHS prototype.

doi:10.18086/eurosun.2022.13.17 Available at http://proceedings.ises.org

The use of passive techniques results in an unchanged storage capacity as the PCM mass remains unaltered (Cao ,2018; Sarı, 2001).

For horizontal shell and tube energy storage unit, Yazici et al.,2014 (Yazici,2014) experimentally studied the effect of vertical relocation of the inner tube on the solidification behavior of paraffin wax. Among all eccentric cases, the results revealed that the concentric tube case had the least solidification time. Pahamli et al.,2016 (Pahamli, 2016) numerically studied the effect of varying each of the eccentricity of a circular inner tube and HTF specifications on the melting behavior of a PCM in shell and tube heat exchanger unit. It was concluded that increasing the inner tube eccentricity caused a reduction in the melting time. Alnakeeb et al.,2021 (Alnakeeb, 2021) studied the effect of eccentricity on the inner tube at different aspect ratios on the melting characteristics of the PCM storage unit. However, the cumulative impact of orientataion and radial eccentricity on thermal characteristics still requires extensive investigation.

The inference from the preceding literature survey is that there is a paucity of research on passive heat transfer augmentation techniques for high-temperature PCM. Hence, the present study numerically investigates the combined effect of the passive heat transfer augmentation techniques on thermal chacteristics of HT-LHS system. The orientation of the domain and radial eccentricity of HTF tube are simultaneously changed to observe the cumulative effect.

2. Problem statement and numerical formulation

2.1. Physical and computational domain

The physical domain of the system comprises of two tubes with HTF running through the inner tube and PCM present in the annulus.The schematic illustration of the computational domain and dimensions of the cross-section of the LHS systems are presented in *Figure 32 (a)*. The inner copper tube has an outer diameter of 26.7 mm and the outer steel shell has an inner diameter of 84.68 mm. The HTF (Therminol VP 1) flows through the copper tube and the annulus contains high-temperature PCM (Binary mixture of $NaNO_3$ and KNO_3). The hot HTF and the cold HTF enters the tube during charging and discharging, respectively. The conjugate heat transfer between PCM and HTF is through combined convection and conduction during charging and discharging. The heat transfer from fluid to outer tube wall is forced convection and melting of PCM generates free convection. Although the specific dimension of the LHS system is selected in this study, the outcomes are applicable for different dimensions and configurations since the thermohydraulic process involving conjugate heat transfer and phase change is similar in concentric tube LHS systems. Two orientations of the domain i.e. horizontal ($\theta = 0^o$) and vertical ($\theta = 90^o$) are considerd to observe the effect of orientation on the heat transfer characteristics. *Figure 3* illustrates the cross section of LHS system for four different radial eccentricity for $\theta = 0^o$ domain. Vertical eccentricity is provided in positive and negative direction ($\theta = 0^o$, $e_x = 0, e_y = c$). The temperature dependent thermophysical properties of the PCM and HTF are presented in Table 1 and Table 2 respectively.

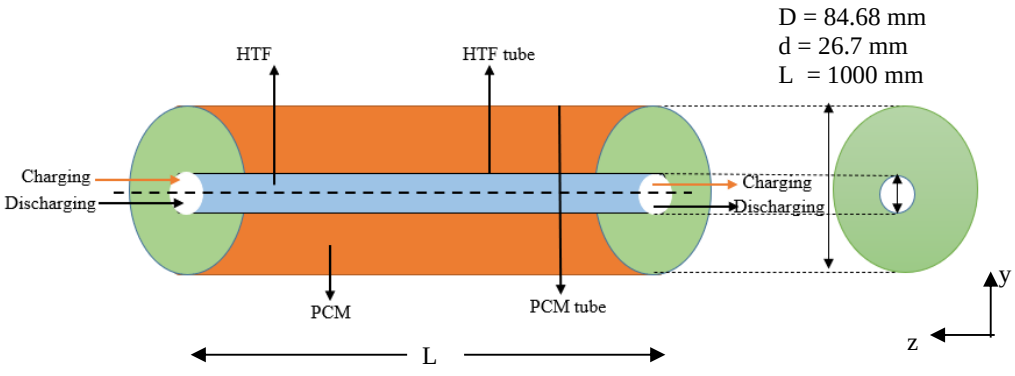

(a)

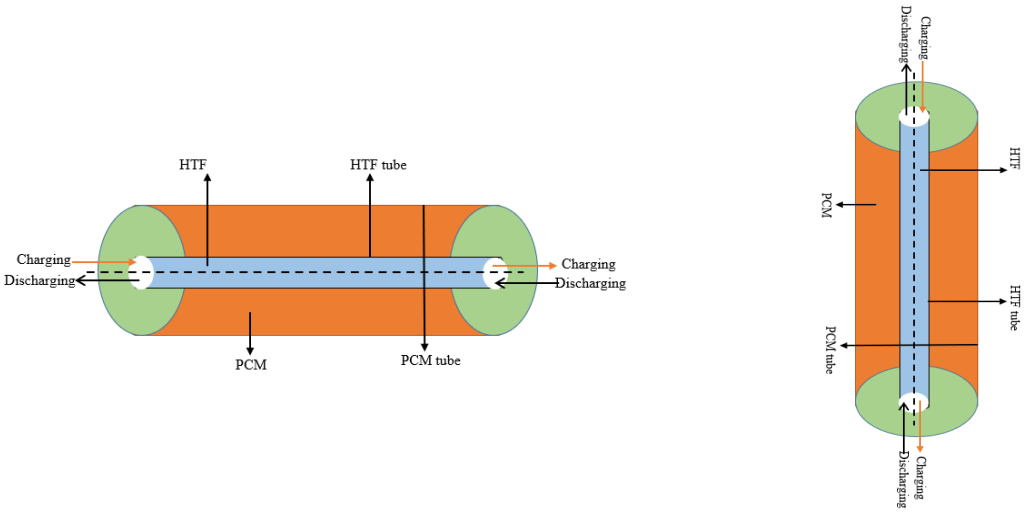

(b) (c)

Figure 2: (a) Dimensions of the physical domain of the concentric LHS system , (b) Horizontal orientation of the LHS domain,and (C) Vertical orientation of LHS domain

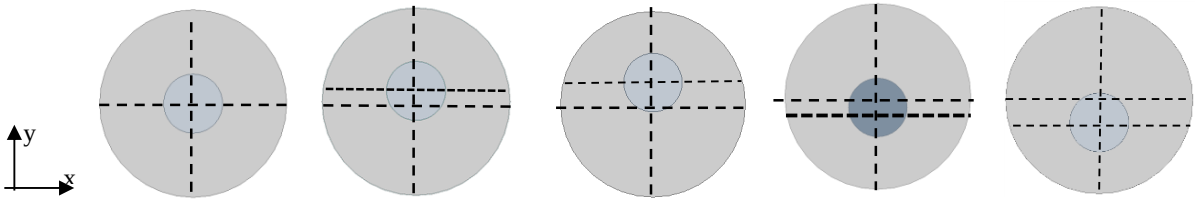

Figure 3: Cross-section of computational domain. (a) Concentric tube ($e_x = e_y = 0$),(b) $e_x = 0$,$e_y = 5$ mm ,(c) $e_y = 0$, $e_y = 10$ mm and (d) $e_x = 0$, $e_y = -5$ mm and (e) $e_x = 0$ mm, $e_y = -10$ mm .

Where e = eccentricity of HTF tube = Distance between center of outer and inner tube

Table 1: Thermophysical properties of PCM

Temperature (K)	Density (kg/m^3)	Specific heat (J/kgK)	Thermal conductivity (W/mK)$\times 10^{-3}$	Viscosity (Pa.s))$\times 10^{-3}$
500	1945	1486	486.5	5.5
550	1913	1495	496.1	3.839
600	1882	1503	505.8	2.707
650	1850	1512	515.6	1.992
700	1818	1520	525.4	1.583

Table 2: Thermophysical properties of HTF

Temperature (^oC)	Density (kg/m^3)	Specific heat (J/kgK)	Thermal conductivity (W/mK)	Viscosity (Pa.s)	Vapor pressure (kPa)
200	913	2048	0.114	0.000395	24
220	895	2101	0.111	0.000345	42
240	877	2154	0.107	0.000305	68
260	857	2207	0.104	0.000272	108
280	838	2260	0.100	0.000244	163
300	817	2314	0.096	0.000221	239

2.2. Numerical formulation

Enthalpy-Porosity technique is employed to investigate the solid-liquid phase change using Ansys Fluent®. The governing equations are formulated while taking the following assumptions into consideration:

- Molted PCM is assumed to be Newtonian and incompressible fluid
- Change in volume during melting is not considered

- Uniform thermophysical properties are considered for both solid and liquid phases
- Tube wall thermal resistance is neglected

The energy conservation equation is formulated as.

$$\frac{\partial(\rho H)}{\partial t} + \nabla.(\rho v H) = \nabla.(k\nabla T) + S_d \quad \text{(eq. 1)}$$

$$H = h_s + \beta\, \Delta H_{fusion} \quad \text{(eq.2)}$$

$$h_s = h_r + \int_{T_r}^{T} c_p dT \quad \text{(eq.3)}$$

Where H is total enthalpy, h_s is sensible enthalpy, δ is melting fraction, S_d is energy dissipation, h_r is sensible enthalpy at reference temperature and ΔH_{fusion} is the latent heat of fusion.

$$\beta\,(T) = \text{liquid fraction} = \begin{cases} 0 & T < T_{solid} \\ \frac{T - T_{solid}}{T_{liquid} - T_{solid}} & T_{solid} \le T \le T_{liquid} \\ 1 & T > T_{liquid} \end{cases} \quad \text{(eq. 4)}$$

Replacing δ in Equation (4), the energy equation can be expressed as:

$$\frac{\partial(\rho h_s)}{\partial t} + \nabla.(\rho v h_s) = \nabla.(k\nabla T) - \frac{\partial(\rho\beta \Delta \text{Hfusion})}{\partial t} - \nabla.(\rho v \beta \Delta \text{Hfusion}) + S_d \quad \text{(eq. 5)}$$

Where T = Local temperature

T_{solid} = Solidus temperature of PCM (K)

T_{liquid} = Liquidus temperature of PCM (K)

A value of δ = 0 corresponds to solid phase and δ = 1 defines liquid phase. Value of 0<δ <1 represents a mushy zone (pseudo porous zone) consisting of both solid and liquid phases.

The momentum equation to include natural convection can be expressed as:

$$\frac{\partial \rho v}{\partial t} + \nabla.(\rho v v) = -\nabla p + \nabla.(\mu \nabla v) + \rho g + M v \quad \text{(eq.6)}$$

$$M(\beta) = \frac{(1-\beta)^2}{\beta^3 + \epsilon} A \quad \text{(eq. 7)}$$

Where M = porosity function and A = Mushy zone constant which reflects the morphology of mushy zone. ϵ is a constant having a small value (0.001). M helps the momentum equation to approximate the Carman-Kozney equations for flow in porous media. 'A' measures the amplitude of velocity damping. The disparity in simulation could be caused by extremely high values of A. 'A' is 10^5 in the present study.

Boussinesq approximation assumes the constant fluid density in all terms of Eqn (6) except the buoyancy force which would generate convection in molten PCM. This body force is modeled using ρ_r and T_r. Hence, the momentum equation can be expressed as:

$$\frac{\partial \rho_r v}{\partial t} + \nabla.(\rho_r v v) = -\nabla p + \nabla.(\mu \nabla v) + (\rho - \rho_r) g + \frac{(1-\beta)^2}{\beta^3 + \epsilon} A v \quad \text{(eq. 8)}$$

$$(\rho - \rho_r) g = -\rho_r k_T (T - T_r) \quad \text{(eq.9)}$$

k_T is the coefficient of thermal expansion of molten PCM and ρ_r, T_r are reference density and temperature respectively.

The continuity equation can be expressed as:

$$\frac{\partial \rho}{\partial t} + \nabla.(\rho \vec{U}) = 0 \quad \text{(eq.10)}$$

As the flow is considered incompressible, the continuity equation can be expressed as

$$\nabla.\vec{U} = 0.$$

The transient simulation with the pressure staggering option (PRESTO) scheme is used for the pressure correction equation, and a SIMPLE algorithm is used for pressure–velocity coupling (Mat et al. 2013). A second order upwind scheme was used to solve the momentum and energy equations. First order implicit scheme is used to discretize the transient term.

2.3 Initial and boundary conditions

At t=0 the PCM is assumed to be at 488 K. HTF is introduced into the tube at temperature and mass flow rate of 525 K and 0.5 kg/s, respectively. Heat transfer from HTF to PCM during charging is simulated using coupled boundary conditions at the inner tube wall. The exterior wall of the shell is assumed to be entirely insulated. Outflow condition is employed at the exit of heat transfer fluid tube.

Mathematically, the mass and energy conservation for this specific problem can be expressed as:

$$\dot{m}_{in} - \dot{m}_{out} = 0 \quad \text{(eq. 11)}$$

$$\dot{E}_{in} - \dot{E}_{out} = \dot{E}_{transfer} \quad \text{(eq. 12)}$$

Where $'\dot{m}_{in}'$ is mass flow of HTF at inlet, $'\dot{m}_{out}'$ is mass flow of HTF at outlet.

3. Results and discussion

3.1 Model verification and validation

The numerical results are verified for grid and time independence before proceeding with the simulation.3D domain is considered for horizontal domain and 2D axisymmetric domain is considered for LHS system with vertical orientation. Figure 4 (a) performs grid independence for three different number of elements with time step of 0.01 s. The results did not alter extensively with an increase in elements from 2,04,918 to 2,44,900. Therefore, the model with 2,04,918 elements with time step 0.025 s is considered to achieve the predetermined convergence level.

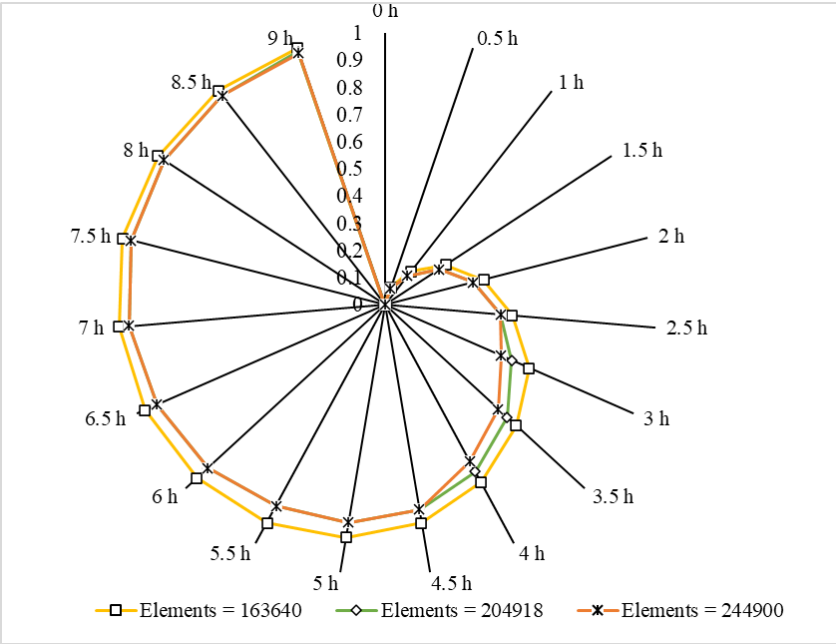

Figure 4: Grid independence test

The numerical model is verified by comparing predictions with previous experimental results from Hosseini et al. (Hosseini, Rahimi, and Bahrampoury 2014) and numerical results from Seddegh et al. (Seddegh, Wang, and Henderson 2016). Figure 5 compares the volumetric average temperature of the PCM domain during charging with the experimental and numerical findings during the charging process. The geometric and operating parameters are kept constant as previus literature to validate the methodology. The volume flow rate of 1 lpm, and inlet temperature of 343 K are considered for the test. The results from the simulation using present numerical technique reflect good agreement with previous results.

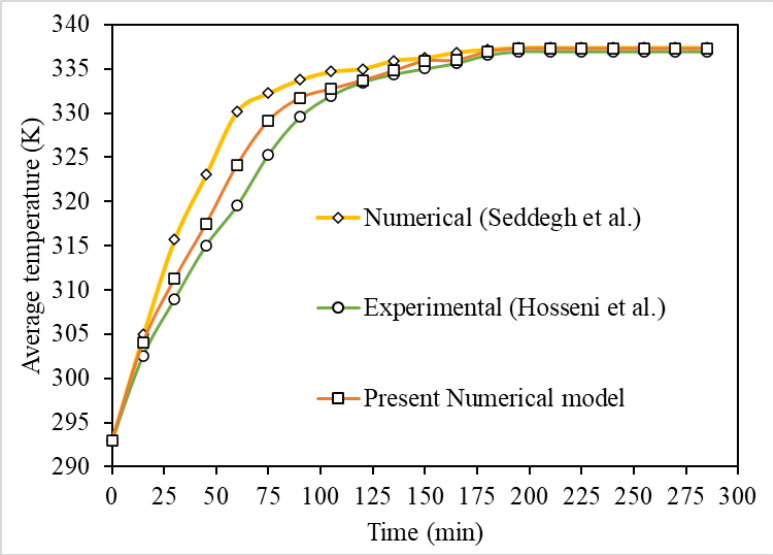

Figure 5: Validation of the present model with experimental and numerical model

3.2 Charging performance comparison between horizontal and vertical domain

Figures 6 (a) and 6 (b) display the liquid fraction and temperature variations respectively for concentric horizontal configuration as shown in Figure 2 (b). At the beginning of charging the solid phase change material in contact with the tube surface absorbs heat from hot heat transfer fluid and subsequently reaches the melting temperature. As a result, the recirculation zone is created in molten PCM, which generates an intense convection current. This intense movement between molten PCM and interface between liquid and solid PCM intensifies the melting. The melted PCM rises to top of the shell side, while solid PCM precipitates because of buoyancy. In the end, the melted PCM filled the upper half of the LHS system as depicted in Figure 6(a).

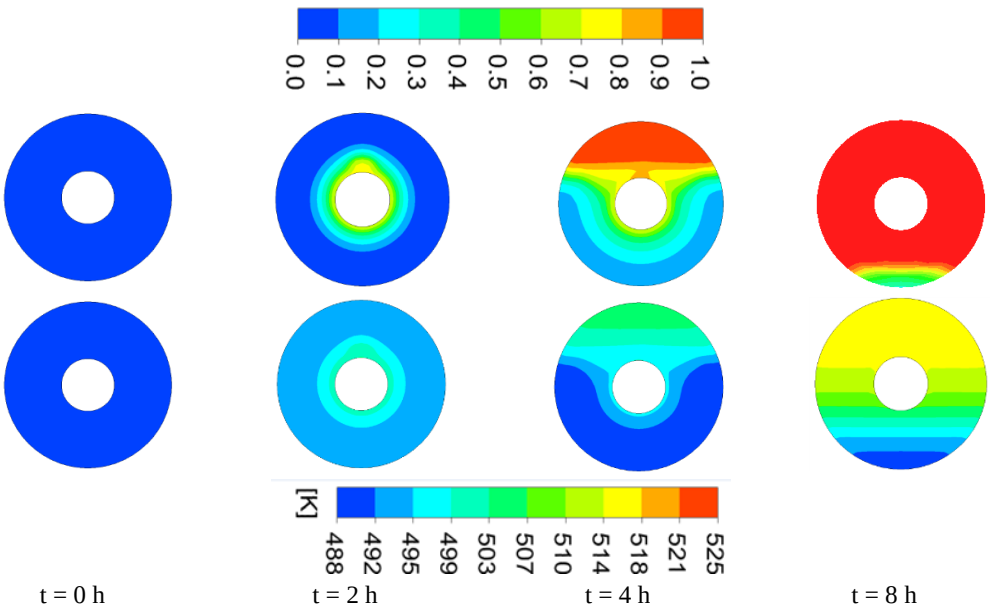

Figure 6: Liquid fraction and temperature contour distribution for horizzontal domain. Upper row: Liquid fraction,and lower row: Temperature

Figures 7 (a) and 7(b) illustrate the contours of liquid fraction and temperature respectively for vertical concentric system present in Figure 2 (c). Likewise horizontal domain, the solid PCM near the heat transfer tube absorbs heat from hot heat transfer fluid. When a layer of melted PCM is formed adjacent to the tube

surface, the melted PCM rises along the outer surface of the tube due to buoyancy. This motion creates a convective current in melted PCM between HTF tube and melted PCM and as well as between the liquid and solid interface. In contrast to horizontal system, the convective current persists and is effective during entire charging process for vertical LHS system. As a result, the vertical LHS system maintains nearly a constant charging rate. Figure 7 (b) displays practically lack of temperature stratification in the melted PCM.

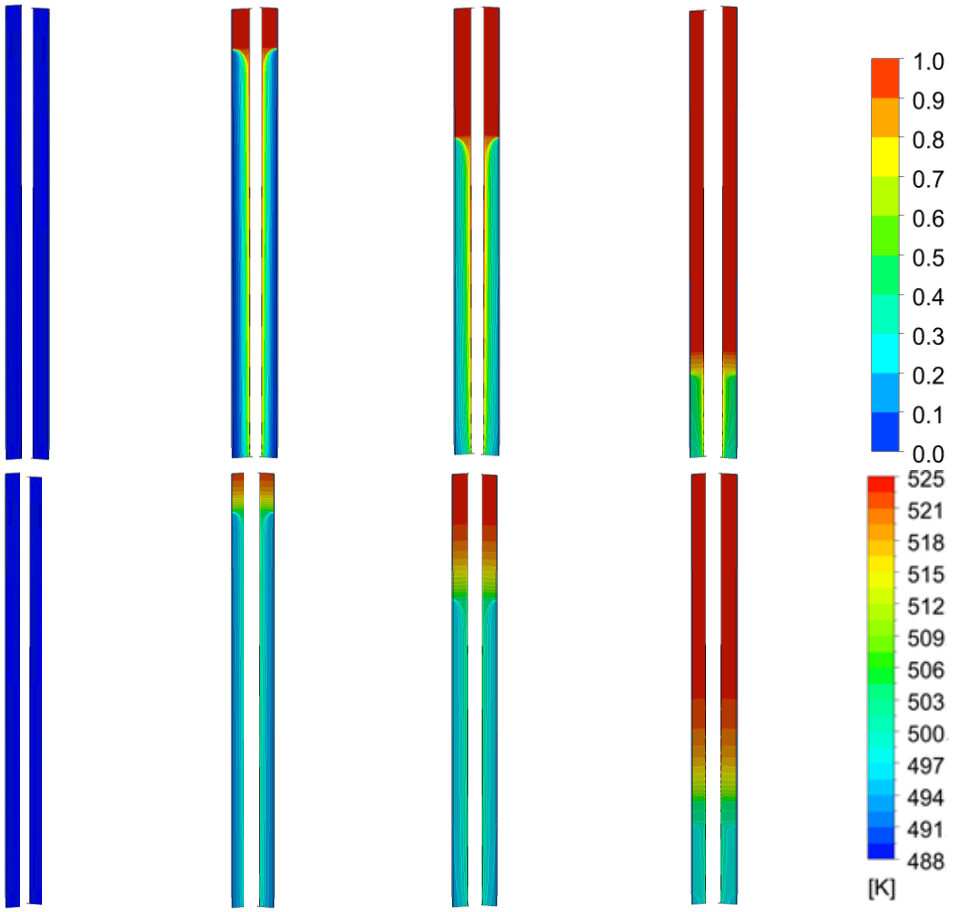

Figure 7: Liquid fraction and temperature contour for vertical domain. Upper: Liquid fraction , and Lower: Temperature

3.3 Combined influence of orientation and eccentricity on charging performance

Figure 8 compares the effect of horizontal and vertical orientation ($\theta = 0^o$ and $\theta = 90^o$) on the charging characteristics for latent heat storage. In the beginning, the rate of melting remains almost the same for both configurations. This can be attributed to the presence of only conduction at the start of the charging process which is independent of θ. A high melting rate during charging refers to the transition in thermal state of PCM from solid to the melted. When melting begins, the recirculation propagates in axial and radial directions in melted medium of the LHS system. For $\theta = 0^o$, the radial component helps to the increase in melting rate, and the axial component facilitates the melting along the length of the horizontal system. On the other hand, the same convective motion persists during the entire charging process in the vertical LHS domain.

Charging duration for LHS should be as small as possible for improved performance. From Figure 8, it is evident that the horizontal domain has superior performance compared to vertical domain. Hence, the horizontal configuration is subjected to change in eccentricity of the HTF tube to evaluate the combined effect.

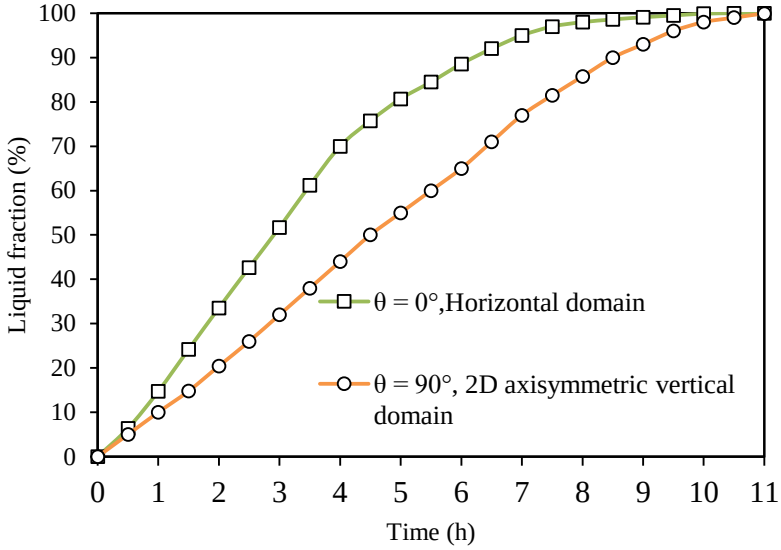

Figure 8: Temporal variation of liquid fraction for θ = 0° and θ = 90°

The degree of eccentricity is varied in both horizontal (e_x = c, $e_{y=0}$) and vertical direction (e_y = c, $e_{x=0}$). Figure 9 represents the liquid fraction and temperature contour for different degree of eccentricity for horizontal domain (**θ = 0°**). At the beginning, there are no difference in charging rate of eccentric tube as compared to concentric tube as visible from Figure 10 which is due to pure conduction heat transfer from inner tube wall to solid PCM. Gradually, temperature of PCM layer adjacent to the inner tube increases first and PCM starts to melt after temperature reaches the melting point. The molten PCM adjacent to lower part of the inner tube moves to upper side of inner tube due to buoyancy. This generates natural convection current in molten PCM which continues to dominate in eccentric system. When the eccentricity of inner tube descends downwards from the coaxial center with the outer tube, the area available for natural convection increases enhancing the melting rate. This can be attributed to the correlation between convective heat transfer with the effective surface area available for natural convection ($\dot{Q} \propto A_{eff}$). The eccentric geometry with e = -20 mm presented the shortest melting time due to enhanced convective heat transfer coefficient. On the contrary, the horizontal eccentricity does not affect the charging rate as buoyancy has no effect on horizontal direction. Table 3 summarizes the percentage of increase or decrease in charging duration corresponding to different configuration of LHS system.

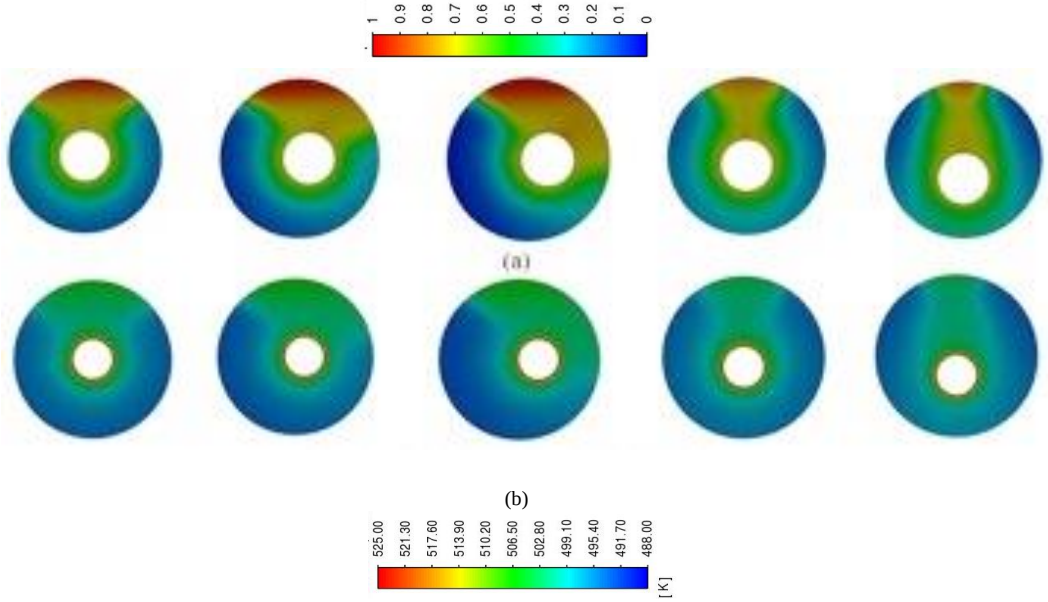

Figure 9: Liquid fraction and temperature distribution after 3 h of charging at z = 0.5 m cross section. (a) Liquid fraction and (b)Temperature

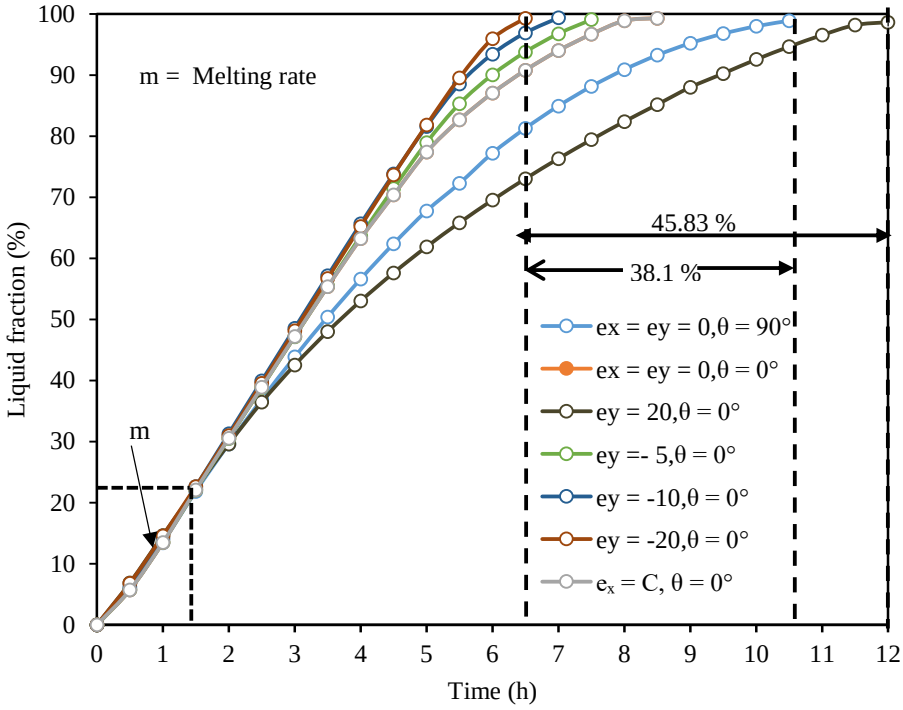

Figure 10: Combined effect of orientation and radial eccentricity on charging performance (e is in mm)

Table 3: Quantitaive illustration of combined effect of passive enehancement techniques

Configuration	Orientation, eccentricity (mm)	Charging duration (hrs)	Change wrt concentric vertical domain (%)
Concentric vertical Vertical	θ = 90°,e = 0	10.5	Reference
Change in orientation	θ = 0°, e = 0	8.5	19.04 ↓
Cumulative impact of orientation and eccentricity (-ve y direction)	θ = 0°, e_y = - 20	6.5	38.09 ↓
Cumulative impact of orientation and eccentricity (+ve y direction)	θ = 0°, e_y = 20	12	14.28 ↑
Cumulative impact of orientation and eccentricity (x direction)	θ = 0°, e_x = C	8.5	19.04 ↓

3.4 Effect of inlet temperatures and flow rates of HTF

From the previous section, horizontal eccentric domain having larger downward eccentricity is observed to have the best charging performance. Hence, a parametric analysis is carried out to evaluate the effect of the inlet temperatures and flow rates of HTF on the charging characteristics of the eccentric domain of θ=0° having downward vertical eccentricity. Three different temperatures at a constant HTF flow rate of 0.5 lpm and three different HTF inlet flow rates at a constant inlet temperature of 525 K are considered.

Figure 11 compares the liquid fraction and temperature of the PCM at different inlet temperatures during charging process. The temperature and liquid fraction are defined as average over the volume of the domain. The melting fraction and temperature menifests energy storage capacity of the LHS system at each instant during charging. The total charging duration is found to decrease with increase in inlet temperature. The reduction is explained by the intensified buoyancy and convective heat transfer in the PCM resulting from the high temperature gradient in the vicinity of the HTF tube. This results in increase in rate of energy transfer to the PCM. Figure 11 also reflects that the total melting time is reduced by 21.56 % and 44.53 % in the horizontal eccentric system as the HTF temperature is increased from 515 K to 520 K and then 530 K. The average temperature of PCM is increased by 1.1 % and 5% respectively as the HTF temperature is increased from 515 K to 520 K and then 530 K.

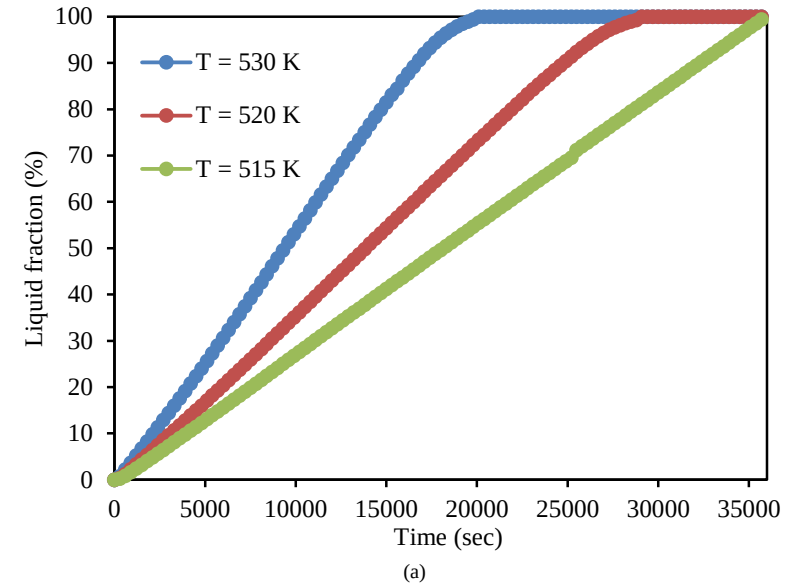

(a)

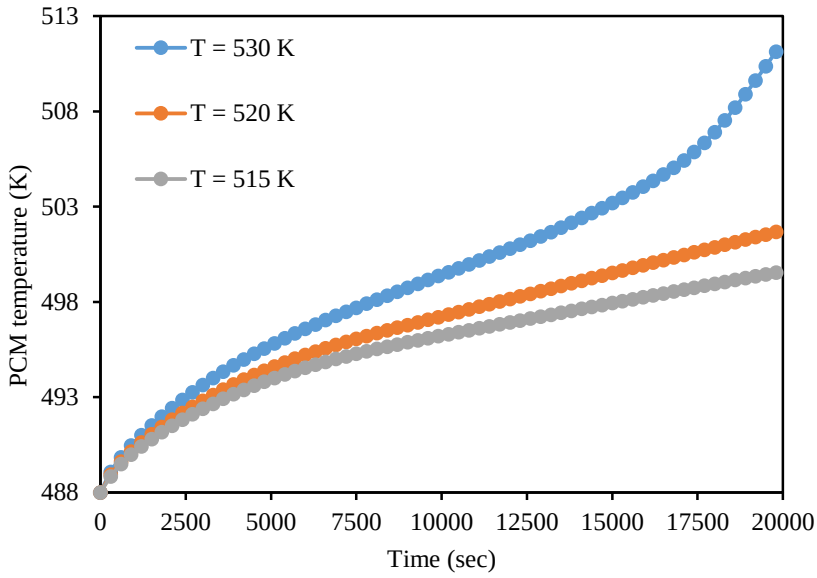

(b)

Figure 11: Thermal performance outputs in horizontal eccentric domain during the charging process. (a) PCM liquid fraction, and (b) PCM temperature

Figure 12 compares the liquid fraction of PCM under different Reynold's number during charging process. The increase of flow rate does not show significant changes in the total melting time during the charging process. This behaviour can be explained by the conjugate heat transfer mechanism from HTF to PCM. Heat transfer between the hot HTF and inner tube surface is by forced convection which has much higher heat transfer coefficient in comparison to natural convection in the liquid PCM. Change in flow rate of HTF affects the forced convection in HTF tube. However, the natural convection dominated heat transfer in the liquid PCM is not significantly affected by flow rate. Therefore, increasing the HTF flow rate has minimal effect on the thermal performance of any orientation.

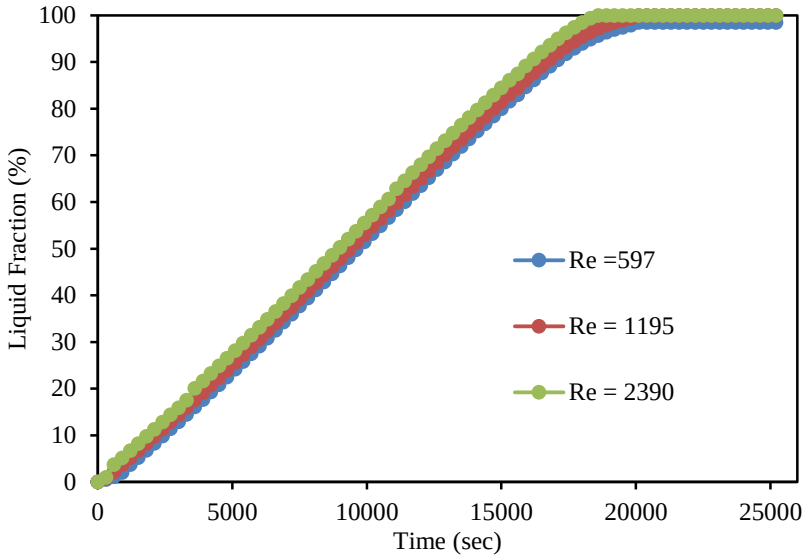

(a)

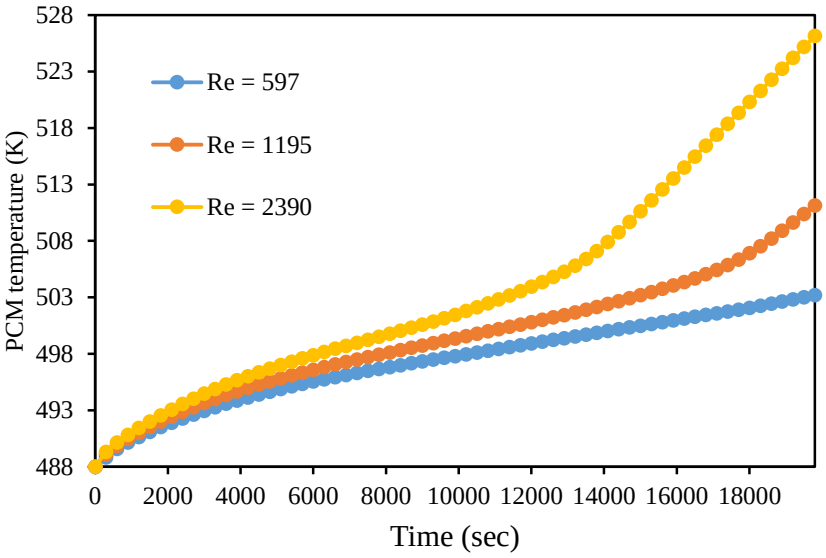

(b)

Figure 12: Thermal performance outputs in horizontal eccentric domain during the charging process. (a) PCM liquid fraction, and (b) PCM temperature

4. Conclusions:

The low heat transfer rate in LHS because of low thermal conductivity of inorganic PCM is the major technological bottleneck in designing HT-LHS systems. There are active and passive heat transfer enhancement methods to improve the heat transfer performance. Passive techniques such as variation in orientation of LHS domain and eccentricity of HTF tube can improve the thermal performance of HT-LHS system. Though individual effect of passive heat transfer enhancement techniques is relatively small compared to active heat transfer enhancement techniques, the combined effect is observed to be significantly large .

Changing the orientation from $\theta = 90°$ to $\theta = 0°$ with no eccentricity results in a 19 % increase in charging rate. Moreover, when both orientation and eccentricity are changed together, the charging rate increases by 38 % from $\theta = 90°$,e = 0 mm to $\theta = 0°$,e = -20 mm . However, if the eccentricity is upward at 20 mm for $\theta = 0°$, the charging rate reduces by 41.12 % than $\theta = 0°$ without eccentricity. The increase in charging (melting) rate with vertical downward eccentricity is atrributed to larger available surface area for natural convection. The substantial increase in rate of charging would help to devise the HT-LHS system with horizontal

orientation and vertical downward ecentricity. The charging duration of eccentric domain with vertical downward eccentricity substantially decreases with increase in inlet temperature of hot HTF. However, the inlet flow rate has minimal impact on charging duration. The future study will consider the effect of combined strategies on discharging performance of HT-LHS system and will explore the intensity of turbulence on hear transfer characteristics.

Acknowledgment: Authors would like to thank UQIDAR to fund this collaberative research work

References

Al-Maghalseh, Maher and Khamid Mahkamov,2018.Methods of Heat Transfer Intensification in PCM Thermal Storage Systems: Review Paper. *Renewable and Sustainable Energy Reviews*, 92,pp.62–94. *https://doi.org/10.1016/j.rser.2018.04.064*.

Alnakeeb, Mohamed A., Mohamed A. Abdel Salam, and Mohamed A. Hassab,2021.Eccentricity Optimization of an Inner Flat-Tube Double-Pipe Latent-Heat Thermal Energy Storage Unit. *Case Studies in Thermal Engineering*, 25,pp.100969. *https://doi.org/10.1016/j.csite.2021.100969*.

Cao, Xiaoling, Yanping Yuan, Bo Xiang, and Fariborz Highlight, 2018.Effect of Natural Convection on Melting Performance of Eccentric Horizontal Shell and Tube Latent Heat Storage Unit. *Sustainable Cities and Society*, 38,pp.571–81. *https://doi.org/10.1016/j.scs.2018.01.025*

Hosseini, M. J., M. Rahimi, and R. Bahrampoury,2014.Experimental and Computational Evolution of a Shell and Tube Heat Exchanger as a PCM Thermal Storage System. *International Communications in Heat and Mass Transfer*, 50,pp.128–36. *http://dx.doi.org/10.1016/j.icheatmasstransfer.2013.11.008*

Jegadheeswaran, S. and Sanjay D. Pohekar, 2009.Performance Enhancement in Latent Heat Thermal Storage System: A Review. *Renewable and Sustainable Energy Reviews*, 13(9),pp.2225–44. *http://doi.org/10.1016/j.rser.2009.06.024*

Mat, Sohif, Abduljalil A. Al-Abidi, K. Sopian, M. Y. Sulaiman, and Abdulrahman Th Mohammad,2013. Enhance Heat Transfer for PCM Melting in Triplex Tube with Internal-External Fins. *Energy Conversion and Management*, 74,pp.223–36. *http://dx.doi.org/10.1016/j.enconman.2013.05.003*

Nazir, Hassan, Mariah Batool, Francisco J. Bolivar Osorio, Marllory Isaza-Ruiz, Xinhai Xu, K. Vignarooban, Patrick Phelan, Inamuddin, and Arunachala M. Kannan, 2019. Recent Developments in Phase Change Materials for Energy Storage Applications: A Review. *International Journal of Heat and Mass Transfer*, 129,pp.491–523. *https://doi.org/10.1016/j.ijheatmasstransfer.2018.09.126*

Pahamli, Younes, Mohammad J. Hosseini, Ali A. Ranjbar, and Rasool Bahrampoury,2016. Analysis of the Effect of Eccentricity and Operational Parameters in PCM-Filled Single-Pass Shell and Tube Heat Exchangers. *Renewable Energy*, 97,pp.344–57. *http://dx.doi.org/10.1016/j.renene.2016.05.090*

Ray, Alok K., Dibakar Rakshit, and K. Ravikumar, 2021. High-Temperature Latent Thermal Storage System for Solar Power: Materials, Concepts, and Challenges. *Cleaner Engineering and Technology*, 4,pp.100155. *https://doi.org/10.1016/j.clet.2021.100155*

Robinson, Adam, 2017. Ultra-High Temperature Thermal Energy Storage. Part 1: Concepts.*Journal of Energy Storage*, 13,pp.277–86. *http://dx.doi.org/10.1016/j.est.2017.07.020*

Sarı, Ahmet and Kamil Kaygusuz, 2001.Thermal Performance of Myristic Acid as a Phase Change Material for Energy Storage Application. *Renewable Energy*, 24(2),pp.303–17.

Seddegh, Saeid, Xiaolin Wang, and Alan D. Henderson,2016. A Comparative Study of Thermal Behaviour of a Horizontal and Vertical Shell-and-Tube Energy Storage Using Phase Change Materials. *Applied Thermal Engineering*, 93,pp.348–58. *http://dx.doi.org/10.1016/j.applthermaleng.2015.09.107*

Yazici, Mustafa Yusuf, Mete Avci, Orhan Aydin, and Mithat Akgun. 2014. On the Effect of Eccentricity of a Horizontal Tube-in-Shell Storage Unit on Solidification of a PCM. *Applied Thermal Engineering*, 64(1–2),pp.1–9. *http://dx.doi.org/10.1016/j.applthermaleng.2013.12.005*

Zablocki, Alexandra. 2019. “Energy Storage: Fact Sheet (2019).” *Eesi* 2040(February):1–8.